Functional Micro-imaging at the Interface of Bone Mechanics and Biology

R. Müller, A. Nazarian, P. Schneider, M. Stauber, P. Thurner, G.H. van Lenthe, R. Voide

Swiss Federal Institute of Technology (ETH) and University of Zürich, Institute for Biomedical Engineering, Switzerland
ralph.mueller@ethz.ch

With recent advances in genetics and molecular medicine there is a strong need for quantitative image processing of three-dimensional (3D) biological structures. A number of new microstructural imaging modalities have been put forward recently, allowing phenotypic quantification with high precision and accuracy in humans and animals; especially in the mouse. Although biomedical imaging technology is now readily available, few attempts have been made to expand the capabilities of these systems by adding quantitative analysis tools as an integrative part of biomedical information technology. New strategies for 3D approaches for quantitative image processing and analysis of biological structures are presented. The focus will be on aspects of bioengineering and biomedical information technology in micro-imaging and image-guided biomechanics.

1 Introduction

Quantitative endpoints have become an important factor for success in basic research and in the development of novel therapeutic strategies in biology and biomedicine. Biomedical imaging of three-dimensional (3D) biological structures has therefore received increased attention for it is often the basis on which both qualitative (i.e. visualization) and quantitative (i.e. morphometry) image processing is performed, especially for the assessment of microstructural properties in small animals (i.e. mice). A number of new imaging modalities have been introduced in recent years. These techniques can typically be used to image a variety of different biological materials ranging from soft to hard tissues. Whereas soft tissue imaging is actually a much larger market and is nowadays regularly used as a standard procedure to image and visualize biological structures, hard tissue (i.e. bone) imaging has made large progress with respect to not only qualitative imaging but also direct 3D quantitative analysis of microstructural images in both human and animal bone.

In this article, strategies for new 3D approaches of quantitative image processing in the study and treatment of osteoporosis and bone loss will be presented. The focus will be on the bioengineering and imaging aspects of osteoporosis research. With the introduction of microstructural imaging systems such as desktop micro-computed tomography (μCT), a new generation of imaging instruments has entered the arena, allowing easy and relatively inexpensive access to the 3D microstructure of bone, and thereby giving researchers a powerful tool for the exploration of age-related bone loss and osteoporosis.

2 Motivation

Osteoporosis, which occurs most frequently in post-menopausal women and the aged, is defined as a systemic skeletal disease characterized by low bone mass and micro-architectural deterioration, with a concomitant increase in bone fragility and fracture risk (Conference (2000)). It is increasingly recognized that osteoporosis is an important public health problem because of the large size of the affected population and the devastating impact of osteoporotic fractures on morbidity and mortality of patients as well as the associated social costs. Expenditure in the United States attributable to osteoporotic fractures in 1995 reached 14 billion dollars (Ray et al. (1997)).

Although many older people may lose bone, not all develop fractures. Bone mineral density, geometry, micro-architecture and quality of the bone material are all components that determine bone strength as defined by the bone's ability to withstand loading. Neuromuscular function and environmental hazards influencing the risk of failing are important factors in determining the fracture risk. As a result, it has been found that, on an individual basis, 10–90% of the variation in the strength of trabecular bone cannot be explained by bone density. Preliminary data have shown that predicting bone strength can be greatly improved by including micro-architectural parameters in the analysis (Turner et al. (1990), Goldstein (1987)).

3 Microstructural Imaging

Quantitative bone morphometry is a method for assessing structural properties of the trabecular bone. Trabecular morphometry has traditionally been assessed in two dimensions (2D), where the structural parameters are either inspected visually or measured from sections, and the third dimension is added on the basis of stereology (Parfitt et al. (1983)). To overcome some of the limitations of 2D histology, several 3D measurement and analysis techniques have been developed over the last two decades. The most common is the use of stereo- or scanning-microscopy to qualitatively assess 3D

microstructure. In using these methods, researchers were able to demonstrate the loss of 3D connectivity with age by visual observation (Mosekilde (1990)). Serial sectioning has been employed to explore the third dimension also quantitatively allowing true measurements of connectivity and other 3D structural properties like volume fraction and surface area (Odgaard (1997)). Nevertheless, being truly destructive, serial sectioning techniques will not allow secondary measurements such as mechanical testing or dynamic histomorphometry.

If we want to define an ideal imaging approach, we would like this imaging modality to be hierarchical, volumetric (3D), multi-contrast (hard vs. soft tissue), and above all fully non-invasive. Hierarchical imaging denotes the ability to resolve anatomical features at a variety of resolutions and size scales using basically the same imaging modality and ideally covering a few orders of magnitude in resolution. This ability will allow measurements starting at the organ level (500 μm resolution; 1000 mm object size), and going down from the structural level (50 μm resolution; 100 mm object size), to tissue level (5 μm resolution; 10 mm object size), and even down to the cell level (0.5 μm resolution; 1 mm object size) using one technology.

Computed tomography is such an approach to image and quantify trabecular bone in three dimensions, providing multi-scale biological imaging capabilities (Fig. 1) with isotropic resolutions ranging from a few millimeters (clinical CT), to few tens of micrometers (μCT) down to one hundred nanometers (synchrotron radiation nanoCT).

The field was pioneered by Feldkamp et al. (1989), who used a microfocus X-ray tube as a source, an image intensifier as a two-dimensional detector, and a cone-beam reconstruction algorithm to create a 3D object with a typical resolution of 50 μm. Others have used synchrotron radiation to get spatial resolutions on the order of micrometers (Bonse et al. (1994)). Where early implementations of microtomography focused more on methodological aspects of the systems and required equipment not normally available to a large public, a more recent development (Rüegsegger et al. (1996)) emphasized the practical aspects of 3D micro-tomographic imaging. The project aimed to enlarge the availability of the technology in basic research and clinical laboratories. This and other similar types of systems, now also commercially available, can be used routinely in basic research and clinical laboratories Also referred to as desktop μCT, they provide nominal resolutions ranging from roughly 5 to 100 μm. Specimens with diameters ranging from a few millimeters to 100 mm can be measured. Desktop μCT is a precise and validated technique (Balto et al. (2000), Kapadia et al. (1998), Müller et al. (1998b)), and has been used extensively for different research projects involving micro-architectural bone (von Stechow et al. (2003), Alexander et al. (2001), Dempster et al. (2001), Turner et al. (2000), Müller and Rüegsegger (1997)) and biomaterials (Lutolf et al. (2003), Zeltinger et al. (2001)). Since the introduction of these systems, there has been an increasing demand for micro-tomographic technology throughout the world.

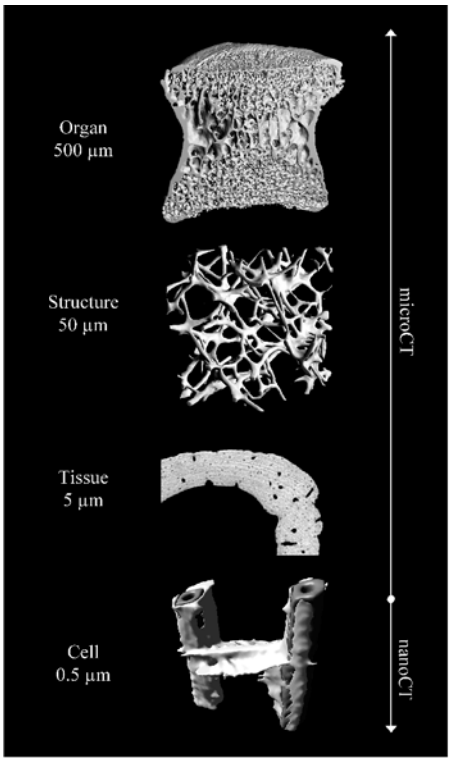

Fig. 1. Schematic overview of hierarchical imaging. From top to bottom: organ, cut through vertebral body demonstrating the large heterogeneity in the vertebra (desktop μCT); structure, three-dimensional representation of the trabecular micro-architecture in a vertebral sample (desktop μCT); tissue, cortical bone sample of a mouse femur illustrating vascular channels (large holes) and cell lacunae (synchrotron radiation μCT, SLS/PSI); osteoblast-like cell stretching between two polymer yarn filaments (synchrotron radiation μCT, SLS/PSI).

4 Three-dimensional Image Processing

Where micro-tomographic imaging provides truly 3D digitizations of the objects of interest, different image processing techniques are actually used for the modeling and analysis of that data. In the following, a few techniques available for the quantification of mineralized bone structures will be discussed.

Surface modeling and reconstruction: for surface modeling and visualization of 3D binary objects, the method described by Lorensen and Cline (1987) is often followed. They developed an algorithm, called marching cubes, which makes it possible to triangulate the surface of any given voxel array very quickly. The marching cubes algorithm is directly applicable to 3D digital data. Using this divide-and-conquer approach, it is not only possible to obtain

a 3D triangular surface representation, but also to effectively smooth the surface. In order to demonstrate the capability of the surface reconstruction algorithm, a series of 3D visualizations are given in Fig. 2, illustrating the large variability in mouse and human bone architectures.

In terms of understanding the basic structure types that exist in trabecular bone, simple models have been proposed. Today, we usually distinguish between rod-like and plate-like structures (Fig. 2(d)–(f). These highly idealized models can be considered as two ends of a spectrum, where the architecture of a real bone specimen will be a mixture of both rods and plates. The prevalence of these types is dependent on the anatomical site as well as the bone age, with typical progression from a plate-like to a rod-like structure. Figure 3 displays three-dimensional, microstructural reconstructions of trabecular bone specimens from four anatomical sites, illustrating very nicely the differences between sites but also the large variance within a given site (Nägele et al. (2004)). Although such 3D visualizations are very helpful and illustrative in describing effects of age and disease on bone architecture, they cannot provide statistically analyzable data.

One method of quantitatively describing bone architecture and the changes associated with age or stage of a disease is the calculation of morphometric indices, also referred to as quantitative bone morphometry. In the past,

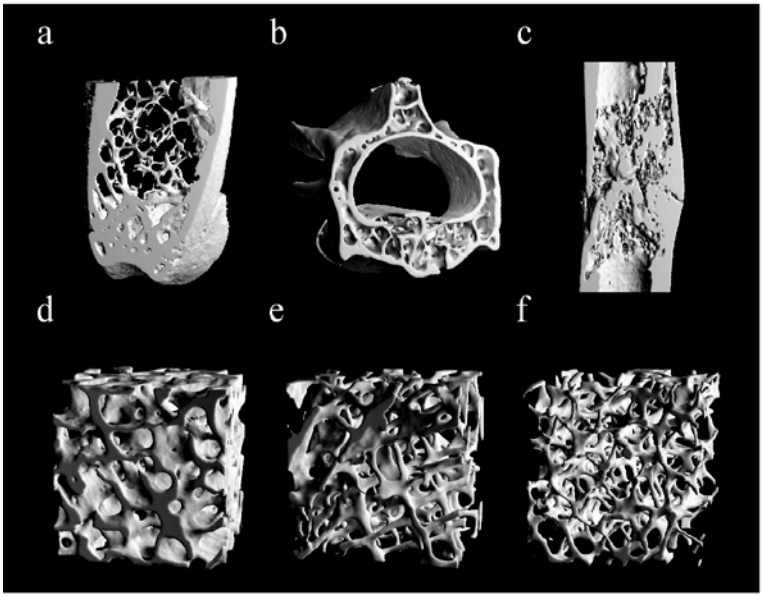

Fig. 2. High-resolution micro-tomographic images from (a) mouse distal femur, (b) mouse lumbar vertebra, (c) mouse femur diaphyseal fracture, (d) human proximal femur (plate-like structure), (e) human iliac crest (hybrid structure), (f) human lumbar spine (rod-like structure).

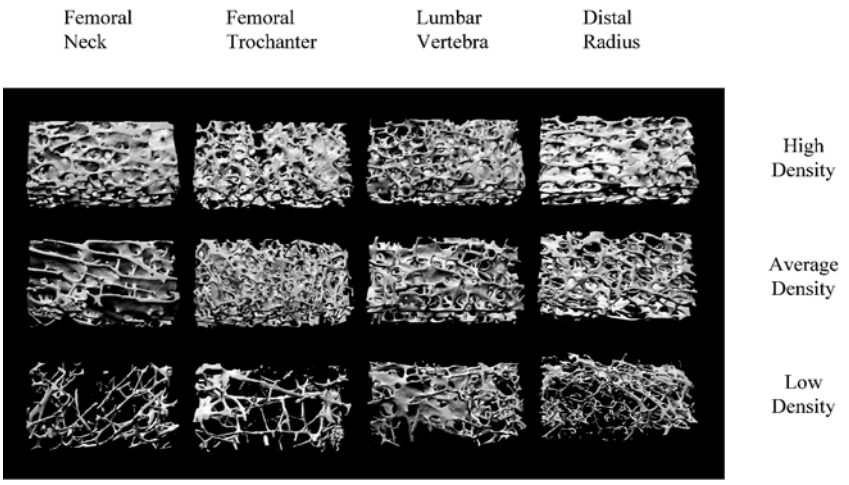

Fig. 3. Three-dimensional micro-tomographic reconstructions of bone autopsies at four different anatomical sites for low, average, and high volume density (data courtesy of Felix Eckstein, Ludwig-Maximilians-University Munich, Germany).

structural properties of trabecular bone have been investigated by the examination of 2D sections of bone biopsies. 3D morphometric parameters were then derived from 2D images using stereological methods (Parfitt et al. (1983)). Highly significant correlations between 2D histology and 3D μCT have been found for bone volume density (BV/TV) and bone surface density (BS/TV) (Müller et al. (1998b)). While measurements like BV/TV and BS/TV can be directly obtained from 2D images, a range of important parameters such as trabecular thickness (Tb.Th), trabecular separation (Tb.Sp), and trabecular number (Tb.N) are derived indirectly assuming a fixed-structure model. Typically, an ideal plate or ideal rod model is used; however, such assumptions are critical due to the fact that trabecular bone architecture differs for different sites and that it continuously changes its structure as a result of remodeling. This has been demonstrated clearly in a large study on 260 human bone biopsies taken from five different skeletal sites, and evaluated with both traditional 2D histomorphometry and newly developed 3D methods (Hildebrand et al. (1999)). For Tb.Th, Tb.Sp and Tb.N, marked differences between the two methods were found, and correlations were only moderate. Furthermore, correlations depended on anatomical site. The latter is caused by anatomical differences in bone architecture; for one site the discrepancy between the true trabecular architecture and the assumed structure is larger than for another site. Hence, deviation from the assumed model will lead to an unpredictable error of the indirectly derived parameters. This is particularly true in studies that follow the changes in bone structure in the course of age-related bone loss, and in evaluating drug therapy. In such cases, a predefined model assumption

could easily overestimate or underestimate the effects of the bone atrophy depending on the assessed index.

For these reasons, and in order to take full advantage of the volumetric measurements, several new 3D image processing methods have recently been presented, allowing direct quantification of bone micro-architecture (Hildebrand et al. (1999), Odgaard (1997)). These techniques calculate actual distances in 3D space and therefore do not rely on an assumed model type and are not biased by possible deviations. In addition to the computation of direct metric parameters, nonmetric parameters can be calculated to describe the 3D nature of a bone structure. An estimate of the plate-rod characteristics can be achieved using the structure model index (SMI). For an ideal plate and ideal rod structure, the SMI is 0 and 3, respectively. For a structure with both plates and rods, the value will be between 0 and 3. Another parameter often used as an architectural index is structural anisotropy (Whitehouse (1974)), a measure of the primary orientation of the trabeculae also often referred to as degree of anisotropy (DA).

The introduction of such direct 3D measures of structural morphometry has added tremendously to the quantitativeness of microstructural imaging. State-of-the-art 3D morphometry is nowadays widely accepted as a gold standard for the characterization of trabecular bone. Nevertheless, new algorithms to better describe the complex nature of bone morphology are currently under development. They typically aim at the better characterization of local bone topology and the assessment of dynamic bone properties as assessed from *in vivo* investigations in humans and animal models of human disease.

5 Experimental Assessment of Bone Competence

Although quantification of bone micro-architecture is of great value in assessing age-related bone loss and the effects of interventions on bone micro-architecture, ultimately the aim of any bone measurement in patients is to assess bone strength. The gold standard to determine bone competence is direct mechanical testing of bone. Although in itself, it is a straightforward procedure, care must be taken in interpreting the results, as they are influenced by anatomical site and loading direction and can be influenced to a large extent by end-artifacts (Keaveny et al. (1997)). Mechanical testing has shown huge heterogeneity in bone mechanical properties, not only across sites and specimens, but even within the same bone these properties can differ 50-fold. Testing also showed that bone is not equally strong in all directions. This mechanical anisotropy is expressed as the ratio of the stiffness in the strongest direction to the stiffness in the weakest direction; it can range from basically 1 (no preferential orientation) to over 10 for both stiffness and strength (Keaveny et al. (2001), Ciarelli et al. (1991)). Because the mechanical behavior of trabecular bone is largely determined by its architecture, many investigators have correlated structural parameters with mechanical properties. Several

studies have shown that where bone density alone explains around 70% of bone elastic properties, by including structural anisotropy the predictive power increases to over 90% (Van Rietbergen et al. (1998), Turner et al. (1990)).

The afore-mentioned studies were all performed on excised bone specimens. In a recent study (Müller et al. (2004)) we showed for the first time that the inclusion of bone architectural indices was also beneficial for the prediction of mechanical competence of whole bones. In that study we evaluated the effect of ibandronate on bone mass, architecture and strength in a large animal study of ovariectomized macaques. Sixty-one adult female macaques were divided into 5 groups ($N = 11$–15): sham control, OVX control, and OVX low-, medium- and high-dose ibandronate. We showed that, in pooled populations, bone mass, as assessed by Bone Mineral Content (BMC), is the single most important predictor for ultimate load ($r^2 = 67\%$). In step-wise multiple regression analysis, Tb.Sp, SMI and BS/BV contributed an additional 21% independently of BMC, such that a total of 88% of the mechano-structure relationship was explained.

6 Computational Assessment of Bone Competence

Although the inclusion of architectural parameters has strongly improved the prediction of strength for bone specimens, they only do so in a statistical sense. They do not explain the real physical contribution of the micro-architecture to the mechanical failure behavior of bone. To understand how differences in bone micro-architecture influence bone strength, insight into load transfer through the bone architecture is needed. With the advent of fast and powerful computers, simulation techniques are becoming popular for investigating the mechanical properties of bone.

Using microstructural finite element (μFE) models generated directly from computer reconstructions of trabecular bone it is now possible to perform a 'virtual experiment', i.e. to simulate a mechanical test in great detail and with high precision. Detailed FE models of trabecular bone can be created using 3D microstructural images, as described before. They are often denoted as 'high-resolution', 'large scale' or 'microstructural' FE models. These models typically represent small trabecular regions in the order of 5 to 10 mm cubes, a scale at which the bone behaves as a continuum. After assigning appropriate material properties to the elements defining the structure, these computer models provide realistic response characteristics to simulated loading. For linear deformation conditions, comparison between biomechanical compression tests and μFE show very good agreement when a homogeneous, isotropic tissue modulus is applied (Kabel et al. (1999), Ladd et al. (1998)). This holds true for normal as well as osteoporotic bone (Homminga et al. (2003)). These computer models allow calculation of loads at the microstructural or even the tissue level (Ladd et al. (1998), Van Rietbergen et al. (1995)) and have been used extensively to accurately determine the apparent mechanical properties of bone specimens.

Recently, it has been shown that non-linear μFE models can accurately predict trabecular bone failure for bovine (Niebur et al. (2000)) as well as human trabecular bone (Bayraktar et al. (2004)) when a bilinear constitutive material model is implemented. After assigning appropriate values for tensile and compressive yield strains, the μFE predicted apparent stresses and strains at failure were equal to experimentally measured values for the same bone specimens, thereby demonstrating that the quality of μFE analyses has reached such accuracy that the use of such simulation techniques can be an effective way to reduce experimental errors (Van Rietbergen et al. (1998)), and can be used as an alternative to destructive mechanical tests (Niebur et al. (2000)). A great advantage of μFE analysis is that the models can be analyzed multiple times under different conditions to simulate various types of loading. Furthermore, bone μFE models provide better insight into the relationship of structure and strength by allowing us to look inside the bone to see where stresses are localizing, and therefore where they may cause fracture.

The μFE models have shown that predicted tissue stresses and strains in the individual trabeculae can differ considerably from those estimated from apparent stresses and strains for the material as a continuum. However, since the *in situ* loading conditions for bone specimens are not precisely known, these models are inadequate for the determination of realistic loading conditions in bone tissue. For the calculation of physiological tissue loading, natural boundary conditions must be applied, which is possible only when μFE models can represent whole bones. Thanks to recent advances in scanning abilities and computer resources, this is now possible. As an example for this approach, the effect of osteoporosis on load transfer in the proximal human femur could be simulated, although at the expense of large computational efforts (Van Rietbergen et al. (2003)). The advantages of these types of analyses are that the complete geometrical and structural organization of a particular bone is taken into account and realistic boundary conditions in modeling the musculoskeletal interface can be applied, such that its outcomes can be directly related to bone failure as a better surrogate for fracture risk. In fact, when the failure characteristics of bone tissue are added to μFE models, the failure process can be followed over time, from local trabecular bone failure to complete fracture (Niebur et al. (2000)).

7 Image-guided Failure Assessment

Thus far, μFE models have mainly assessed bone loading in the elastic range, based on the notion that bone strength is highly correlated with its elastic properties. However, bone fracture is a time-dependent, non-linear event including high local deformations and local trabecular fractures. Although some work on bone failure characteristics has been done, basic knowledge of local trabecular failure is still lacking. In estimating the risk of spontaneous fractures, an extended understanding of the failure behavior of trabecular bone

is essential. For this reason, our group has developed an image-guided failure assessment technique, allowing direct time-lapsed 3D visualization and quantification of fracture progression on the microscopic level (Nazarian and Müller (2004), Müller et al. (1998a)). This technique has recently been validated as compared to classical continuous mechanical testing (Nazarian and Müller (2004)). In order to compute local displacements and strains in the compressed structures a novel image analysis approach has been developed (Müller et al. (2002)). This new method uses sequential structural images from step-wise micro-compression testing to: first, align all images from the different steps; second, identify local anatomical features (nodes) in the structure that can be followed directly in the structure throughout all the steps (Fig. 4(a)); third, create a network of connections between those nodes by image decomposition (Fig. 4(b)); fourth, to compute nodal displacements and local strains between the nodes. In an initial study, trabecular bone specimens were compressed in steps of 0%, 1%, 2%, 4%, 8%, and 12% and local strains were determined experimentally. The method was verified using images, which contained only translations or a uniform stretch in the direction of compression. For the translation, our method predicted the correct translations and the computed strains were zero, as expected. For the uniformly stretched images, we computed strain averages close to the stretch factor ($< 1\%$ error) with a standard deviation of about 10%. For the actual bone micro-compression tests, the results showed that average strains were much smaller than the externally applied strain, but maximum local strain values were 5 to 8 times greater than the externally applied strain, thus providing further evidence for a band-like, local failure behavior of trabecular bone (Fig. 5).

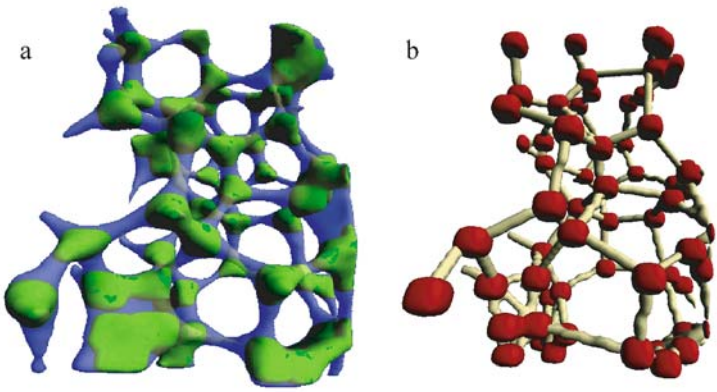

Fig. 4. Three-dimensional image decomposition: (a) thresholded reconstruction of trabecular bone structure with volumetric nodes already identified; (b) topological classification algorithm allows identification of each individual trabecula providing an element node and connection list.

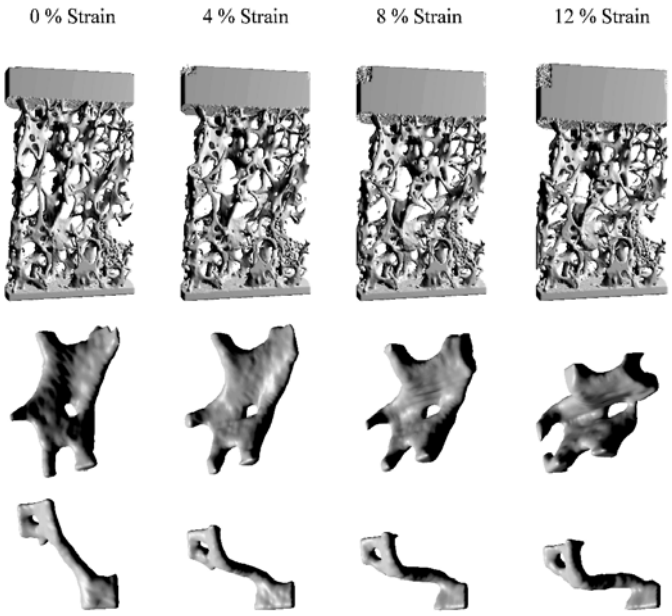

Fig. 5. Failure assessment in a human spine sample using time-lapsed tomographic imaging. Upper row shows a compressed specimen, imaged in steps of 4% strain. Middle and lower rows show how micro-compression can be used to non-invasively monitor the deformation of individual plates and rods, respectively.

These strains were found in rod-like elements that were aligned with the main strain axis. Some of these elements bend, others buckle, and some are compressed. Although inter-node strains can indicate active structure elements, they cannot distinguish the different behavior of these elements and how much energy is absorbed. They also do not correlate well with the amount of deformation in an element. Therefore, inter-node strains alone cannot fully explain the failure mechanisms of trabecular bone. Nevertheless, it is also important to note that failure behavior might be quite different for bone in an *in vivo* environment where boundary conditions differ significantly from *in vitro* setups. Therefore, extrapolation of the results on the material level to the *in vivo* situation in whole bones might prove to be difficult and will have to be addressed in future studies of whole bone failure behavior including not only trabecular micro-architecture but also cortical bone.

Image-guided failure assessment has shown that failure of an individual trabecula can lead to global bone failure; hence, bone failure can be best predicted using a 'weakest link of the chain' approach (Müller et al. (1998a)). Local bone morphometry allows identification of 'weak' trabeculae and therefore improves the predictive ability to determine bone strength and failure

behavior. A 10% change in local thickness (in the rods only) was found to be responsible for a three-fold increase in the mechanical strength of osteoporotic bone, where changes in bone density were only linearly related to bone strength. This might explain a number of findings where only small changes in bone density can achieve up to a 70% reduction in the incidence of fracture. If it were possible to preferentially treat the weakest links of the structure, a minor increase in individual element quality may be enough to prevent a fracture rather than large quantities of new bone. However, this idea is momentarily purely speculative since there are no data from treated patients yet, although it will be possible to obtain such data from iliac bone samples of real patients undergoing treatment. The ability to analyze the same bone sample using both non-invasive micro-architectural imaging and mechanical testing is likely to cause a revival in the use of iliac bone biopsies in the initial assessment of therapeutic success and the regulatory approval of new drugs.

Alternatively, high-resolution *in vivo* imaging modalities are currently under investigation allowing micro-architectural measurements in live patients with resolutions better than 100 μm (Müller (2003)). Although currently only peripheral imaging systems (i.e. measures at the forearm) can achieve this kind of resolution in patients, there is hope that in the future also more central sites such as spine and hip might become accessible to such investigations. This will allow following transient changes in bone micro-architecture in individual patients, giving the clinician a powerful tool for better diagnosis of diseases and online monitoring of treatment regimens.

8 Conclusions

Micro-architectural bone imaging is a nondestructive, non-invasive, and precise procedure that allows the measurement of trabecular and compact bone as well as the repetitive 3D assessment and computation of microstructural and micromechanical properties in patients. The procedure can help improve predictions of fracture risk, clarify the pathophysiology of skeletal diseases, and define the response to therapy. Hierarchical bioimaging in combination with biocomputational approaches are well suited for investigating structure-function relationships as well as failure mechanisms in normal, osteoporotic and treated bone. We expect these findings to improve our understanding of the influence of densitometric, morphological but also loading factors in the etiology of spontaneous fractures of the hip and the spine. Eventually, this improved understanding may lead to more successful approaches in the prevention of such age- and disease-related fractures.

Acknowledgements. These studies were partly funded by a Biomedical Engineering Research Grant of the Whitaker Foundation and the SNF Professorship in Bioengineering of the Swiss National Science Foundation (FP

620-58097.99). We would like to thank Dr. Marco Stampanoni for his support in setting up the tomography station at the MS beamline, Swiss Light Source, PSI, Switzerland.

References

Alexander, J. M., Bab, I., Fish, S., Müller, R., Uchiyama, T., Gronowicz, G., Nahounou, M., Zhao, Q., Chorev, M., Gazit, D., and Rosenblatt, M. (2001). Human parathyroid hormone 1-34 reverses bone loss in ovariectomized mice. *J. Bone Miner. Res.* 16:1665–1673.

Balto, K., Müller, R., Carrington, D. C., Dobeck, J., and Stashenko, P. (2000). Quantification of periapical bone destruction in mice by micro-computed tomography. *J. Dent. Res.* 79:35–40.

Bayraktar, H. H., Morgan, E. F., Niebur, G. L., Morris, G. E., Wong, E. K., and Keaveny, T. M. (2004). Comparison of the elastic and yield properties of human femoral trabecular and cortical bone tissue. *J. Biomech.* 37:27–35.

Bonse, U., Busch, F., Gunnewig, O., Beckmann, F., Pahl, R., Delling, G., Hahn, M., and Graeff, W. (1994). 3D computed X-ray tomography of human cancellous bone at 8 microns spatial and $10^{(-4)}$ energy resolution. *Bone Miner.* 25:25–38.

Ciarelli, M. J., Goldstein, S. A., Kuhn, J. L., Cody, D. D., and Brown, M. B. (1991). Evaluation of orthogonal mechanical properties and density of human trabecular bone from the major metaphyseal regions with materials testing and computed tomography. *J. Orthop. Res.* 9:674–682.

Conference, C. D. (2000). Osteoporosis prevention, diagnosis, and therapy. In *NIH consensus statement*, volume 17, 1–45.

Dempster, D. W., Cosman, F., Kurland, E. S., Zhou, H., Nieves, J., Woelfert, L., Shane, E., Plavetic, K., Müller, R., Bilezikian, J., and Lindsay, R. (2001). Effects of daily treatment with parathyroid hormone on bone microarchitecture and turnover in patients with osteoporosis: a paired biopsy study. *J. Bone Miner. Res.* 16:1846–1853.

Feldkamp, L. A., Goldstein, S. A., Parfitt, A. M., Jesion, G., and Kleerekoper, M. (1989). The direct examination of three-dimensional bone architecture in vitro by computed tomography. *J. Bone Miner. Res.* 4:3–11.

Goldstein, S. A. (1987). The mechanical properties of trabecular bone: dependence on anatomic location and function. *J. Biomech.* 20:1055–1061.

Hildebrand, T., Laib, A., Müller, R., Dequeker, J., and Rüegsegger, P. (1999). Direct three-dimensional morphometric analysis of human cancellous bone: microstructural data from spine, femur, iliac crest, and calcaneus. *J. Bone Miner. Res.* 14:1167–1174.

Homminga, J., McCreadie, B. R., Weinans, H., and Huiskes, R. (2003). The dependence of the elastic properties of osteoporotic cancellous bone on volume fraction and fabric. *J. Biomech.* 36:1461–1467.

Kabel, J., Van Rietbergen, B., Dalstra, M., Odgaard, A., and Huiskes, R. (1999). The role of an effective isotropic tissue modulus in the elastic properties of cancellous bone. *J. Biomech.* 32:673–680.

Kapadia, R. D., Stroup, G. B., Badger, A. M., Koller, B., Levin, J. M., Coatney, R. W., Dodds, R. A., Liang, X., Lark, M. W., and Gowen, M. (1998). Applications of micro-CT and MR microscopy to study pre-clinical models of osteoporosis and osteoarthritis. *Technol. Health Care* 6:361–372.

Keaveny, T. M., Pinilla, T. P., Crawford, R. P., Kopperdahl, D. L., and Lou, A. (1997). Systematic and random errors in compression testing of trabecular bone. *J. Orthop. Res.* 15:101–110.

Keaveny, T. M., Morgan, E. F., Niebur, G. L., and Yeh, O. C. (2001). Biomechanics of trabecular bone. *Ann. Rev. Biomed. Eng.* 3:307–333.

Ladd, A. J., Kinney, J. H., Haupt, D. L., and Goldstein, S. A. (1998). Finite-element modeling of trabecular bone: comparison with mechanical testing and determination of tissue modulus. *J. Orthop. Res.* 16:622–628.

Lorensen, W. E., and Cline, H. E. (1987). Marching cubes: A high resolution 3D surface construction algorithm. *Computer Graphics* 21:163–169.

Lutolf, M. P., Weber, F. E., Schmoekel, H. G., Schense, J. C., Kohler, T., Müller, R., and Hubbell, J. A. (2003). Repair of bone defects using synthetic mimetics of collagenous extracellular matrices. *Nat. Biotechnol.* 21:513–518.

Van Rietbergen, B., Weinans, H., Huiskes, R., and Odgaard, A. (1995). A new method to determine trabecular bone elastic properties and loading using micromechanical finite-element models. *J. Biomech.* 28:69–81.

Van Rietbergen, B., Odgaard, A., Kabel, J., and Huiskes, R. (1998). Relationships between bone morphology and bone elastic properties can be accurately quantified using high-resolution computer reconstructions. *J. Orthop. Res.* 16:23–28.

Van Rietbergen, B., Huiskes, R., Eckstein, F., and Rüegsegger, P. (2003). Trabecular bone tissue strains in the healthy and osteoporotic human femur. *J. Bone Miner. Res.* 18:1781–1788.

von Stechow, D., Balto, K., Stashenko, P., and Müller, R. (2003). Three-dimensional quantitation of periradicular bone destruction by micro-computed tomography. *J. Endod.* 29:252–256.

Mosekilde, L. (1990). Consequences of the remodelling process for vertebral trabecular bone structure: a scanning electron microscopy study (uncoupling of unloaded structures). *Bone Miner.* 10:13–35.

Müller, R., and Rüegsegger, P. (1997). Micro-tomographic imaging for the nondestructive evaluation of trabecular bone architecture. *Stud. Health Technol. Inform.* 40:61–79.

Müller, R., Gerber, S. C., and Hayes, W. C. (1998a). Micro-compression: a novel technique for the nondestructive assessment of local bone failure. *Technol. Health Care* 6:433–444.

Müller, R., Van Campenhout, H., Van Damme, B., Van der Perre, G., Dequeker, J., Hildebrand, T., and Rüegsegger, P. (1998b). Morphometric analysis of human bone biopsies: a quantitative structural comparison of histological sections and micro-computed tomography. *Bone* 23:59–66.

Müller, R., Boesch, T., Jarak, D., Stauber, M., Nazarian, A., Tantillo, M., and Boyd, S. K. (2002). Micro-mechanical evaluation of bone microstructures under load. In Bonse, U., ed., *Developments in X-Ray Tomography III.* San Diego, CA: SPIE. 189–200.

Müller, R., Hannan, M., Smith, S. Y., and Bauss, F. (2004). Intermittent ibandronate preserves bone quality and bone strength in the lumbar spine after 16 months of treatment in the ovariectomized cynomolgus monkey. *J. Bone Miner. Res.* 19:1787–1796.

Müller, R. (2003). Bone microarchitecture assessment: current and future trends. *Osteoporos. Int.* 14 (Suppl. 5):89–99.

Nägele, E., Kuhn, V., Vogt, H., Linka, T. M., Müller, R., Lochmüller, E. M., and Eckstein, F. (2004). Technical considerations for microstructural analysis of human trabecular bone from specimens excised from various skeletal sites. *Calcif. Tissue Int.* 75:15–22.

Nazarian, A., and Müller, R. (2004). Time-lapsed microstructural imaging of bone failure behavior. *J. Biomech.* 37:55–65.

Niebur, G. L., Feldstein, M. J., Yuen, J. C., Chen, T. J., and Keaveny, T. M. (2000). High-resolution finite element models with tissue strength asymmetry accurately predict failure of trabecular bone. *J. Biomech.* 33:1575–1583.

Odgaard, A. (1997). Three-dimensional methods for quantification of cancellous bone architecture. *Bone* 20:315–328.

Parfitt, A. M., Mathews, C. H., Villanueva, A. R., Kleerekoper, M., Frame, B., and Rao, D. S. (1983). Relationships between surface, volume, and thickness of iliac trabecular bone in aging and in osteoporosis. implications for the microanatomic and cellular mechanisms of bone loss. *J. Clin. Invest.* 72: 1396–1409.

Ray, N. F., Chan, J. K., Thamer, M., and Melton 3rd, L. J. (1997). Medical expenditures for the treatment of osteoporotic fractures in the united states in 1995: report from the national osteoporosis foundation. *J. Bone Miner. Res.* 12:24–35.

Rüegsegger, P., Koller, B., and Müller, R. (1996). A microtomographic system for the nondestructive evaluation of bone architecture. *Calcif. Tissue Int.* 58:24–29.

Turner, C. H., Cowin, S. C., Rho, J. Y., Ashman, R. B., and Rice, J. C. (1990). The fabric dependence of the orthotropic elastic constants of cancellous bone. *J. Biomech.* 23:549–561.

Turner, C. H., Hsieh, Y. F., Müller, R., Bouxsein, M. L., Baylink, D. J., Rosen, C. J., Grynpas, M. D., Donahue, L. R., and Beamer, W. G. (2000). Genetic regulation of cortical and trabecular bone strength and microstructure in inbred strains of mice. *J. Bone Miner. Res.* 15:1126–1131.

Whitehouse, W. J. (1974). The quantitative morphology of anisotropic trabecular bone. *J. Microscopy* 101:153–168.

Zeltinger, J., Sherwood, J. K., Graham, D. A., Müller, R., and Griffith, L. G. (2001). Effect of pore size and void fraction on cellular adhesion, proliferation, and matrix deposition. *Tiss. Engrg.* 7:557–572.